



Machining error decomposition and compensation of complicated surfaces by EMD method

Yueping Chen, Hui Tang*, Qingchun Tang, Anshe Zhang, Dawei Chen, Kehui Li

School of Mechanical Engineering, Guangxi University of Science and Technology, Liuzhou, Guangxi Province, China

ARTICLE INFO

Keywords:

Surface parts
empirical mode decomposition (EMD)
Machining errors
Error compensation

ABSTRACT

Complex surface parts are widely used in aerospace, automotive, and precision molds. Modern manufacturing aims to improve the machining accuracy and efficiency of these parts. The machining accuracy of surface parts can be significantly improved using a series of error compensation technologies to compensate for machining errors. Based on the analysis of the measurement data of the parts, empirical mode decomposition (EMD) method is used to decompose the machining errors into systematic and random errors, which are used to modify the numerical control (NC) codes to compensate for the systematic errors of the surface parts. An example of a complicated surface part proves that the method proposed in the current study can effectively improve the machining accuracy of surface parts.

1. Introduction

The applications of complex surfaces increase with the rapid development of modern technology, and modern manufacturing industry requires highly precise applications. The computer numerical control machining accuracy of complex surfaces is affected by various factors, such as manufacturing system, vibration tool size, machine tool thermal deformation, programming, and machining method errors, as well as machine tool deformation. Machining errors must be compensated to improve machining accuracy. Researchers conducted in-depth research on the compensation of machining errors. Topal et al. [1] studied the numerical control (NC) process, suggested a prediction method to solve the cutting force caused by the radial deformation of a workpiece, established the relationship between the cutting force and the deformation of the empirical formula, and compensated errors off-line. Cheng et al. [2] proposed a new geometric error compensation method based on the Floyd algorithm and the product of exponential screw theory. Based on the topological structure and the measured data, the volumetric geometric error modeling was established by the product of exponential screw theory. The improved Floyd minimum distance method was used to build the error compensation model by adjusting weight. The Floyd method was proven to improve the machining precision of a machine. Cho et al. [3] developed a complex surface profile online inspection system and proposed a machining error compensation method based on online measurement technology. Cho combined polynomial neural network algorithm and data inspection method in a model to calculate machining errors under machining conditions and

used an iterative algorithm to modify the tool path to complete error compensation. The validity of the method is verified by experiments. Poniatowska et al. [4] proposed a regression analysis and spatial statistical method to determine the CAD machining pattern model. The offline correction NC code is then used to compensate for the systematic errors of NC machining. The results indicate the significance of compensation effect and efficiency. Wei et al. [5] established a comprehensive mathematical model of geometric and thermal errors, used the CNC system coordinate offset function, and applied a self-developed integrated error real-time compensation system. Errors are compensated online in real time. The results indicate a satisfactory effect, although the NC codes and soft hardware are unchanged by the method. Chen et al. [6] integrated online inspection and compensation and used spatial statistical analysis to process the residuals of the surface regression model to decompose systematic and random errors; systematic errors are compensated online.

Two kinds of machining errors compensation methods exist. The first type is based on error source analysis and compensation. Machining errors are calculated and compensated according to error source modeling. The other type is based on the part measurement data to be analyzed and compensated. Machining errors are calculated and compensated appropriately by comparing the measured surface with the theoretical surface. However, studies on error compensation for complex surface parts based on the empirical mode decomposition (EMD) are scarce. Based on part measurement data analysis, EMD is used in the current study to decompose machining errors. Machining errors are decomposed into systematic and random errors, and the

* Corresponding author.

E-mail address: 893214549@qq.com (H. Tang).

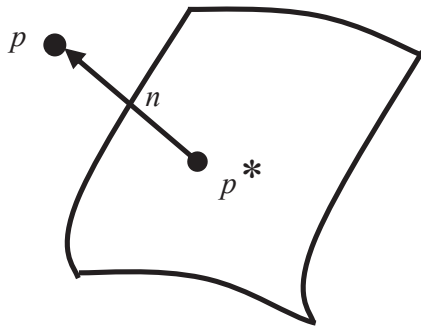


Fig. 1. Minimum distance from a point to the surface.

systematic errors of the machined part are compensated appropriately. The method exhibits the remarkable effects of improving the machining precision of surface parts.

2. Complex surface machining error description

Some differences are observed between the processed part and theoretical surfaces in the NC machining process because of the error sources. These differences are called machining errors. The machining errors of complex surfaces are generally described by the errors of the theoretical points on the surface along the normal vector directions. The normal distances between the machining and theoretical surfaces can be converted to the minimum distances from the actual measuring points to the theoretical surface. Assuming that the coordinates of the measured point are $p(X_A, Y_A, Z_A)$, the corresponding normal is n , and n intersects the theoretical surface at point p^* , which is the corresponding measured point on the theoretical surface. Assuming that the coordinates of the theoretical point is $p^*(X_T, Y_T, Z_T)$, the distance between p and p^* is the minimum distance from measured point p to the theoretical surface (surface machining errors). Fig. 1 shows that surface machining error can be expressed as

$$\varepsilon = \sqrt{(X_A - X_T)^2 + (Y_A - Y_T)^2 + (Z_A - Z_T)^2} \quad (1)$$

where ε is the machining error at each point on the surface; X_T, Y_T, Z_T are the coordinate values of theoretical point p^* ; X_A, Y_A, Z_A are the coordinate values of measured point p . The sign convention in this paper is that machining errors caused by undercutting are denoted as positive errors and the errors caused by overcutting are denoted as negative errors.

In the surface part machining, machining errors are difficult to avoid and the machining errors of the curved surface become a persistent problem because of the influence of error factors. Machining errors can be decomposed into systematic and random errors by considering the measurement data from the surface part. Machining accuracy can be improved after part re-machining by compensating the systematic errors. Therefore, machining errors can be analyzed and compensated by integrating all error factors. Practical applications verify that under certain process conditions, the combined effects of various error sources lead to machining errors, and the effects exhibit a certain degree of stability and repeatability. The differences between the machined surface and the theoretical surface include size, shape, and microscopic errors, such as surface roughness errors. The surface of the machined surface part is measured, and the measured data are reconstructed in the current study to obtain the new surface, which is compared with the theoretical surface to identify deviations. When machining reference is unchanged, the differences can be regarded as machining errors.

In theory, machining errors are the sum of random and systematic errors. Machining errors are directly compensated for in most studies. However, the compensation process is faulty because random errors are difficult to compensate for. Systematic errors are generally larger than

random errors. Thus, compensating for systematic errors can solve the main problem. Only the systematic errors in machining errors are compensated in this study to solve the key problem of compensation errors. Therefore, the two types of errors must be decomposed.

3. Machining error decomposition based on the empirical mode method

To decompose the machining errors, a machining error decomposition method based on EMD is presented in the current study. The systematic and random errors in the machining errors of a part can be decomposed by EMD successfully, and the systematic errors can be compensated.

3.1. Empirical mode decomposition

The EMD [7] is a signal-processing method proposed by Huang et al. of the National Aeronautics and Space Administration. EMD is data-based with good adaptive linear characteristics. Thus, EMD is theoretically applicable to any type of signal decomposition, especially for non-linear and non-stationary signals. Therefore, EMD method is widely used in astronomy, oceanography, biology, earth science, and civil engineering [8–11] but has limited use in mechanical engineering, especially in machining error analysis.

EMD decomposes arbitrary signals into one or several intrinsic modal functions (IMF), and the intrinsic modal function obtained through decomposition satisfies the following constraints:

- (1) The numbers of extreme and zero-crossing points in the entire data sequence is at most one;
- (2) At any point in time, the mean value of the upper and under envelopes determined by the signal maxima and minima, respectively, is zero.

EMD decomposes the fluctuation or trend in different scales step-by-step. A series of data sequences with different characteristic scales is generated. The resulting data sequence is IMF [12]. The EMD decomposition of signal data $x(t)$ is essentially a “sifting” process. The combination of this method with the actual data decomposition process is summarized below. Fig. 2 presents the accelerated speed response of a mechanical gear vibration test.

- (1) First, all extreme points on $x(t)$ must be identified, and all maximum and minimum points must fit into the upper and lower envelopes of $x(t)$ (As indicated by the dashed lines in Fig. 2) by using the cubic spline interpolation function. The upper and lower envelopes should contain all signal data. The average of the upper and lower envelopes is designated as m_1 (As indicated by the thick solid line in Fig. 2). The difference between $x(t)$ and m_1 is defined as h_1 , i.e.

$$x(t) - m_1 = h_1 \quad (2)$$

h_1 should be an IMF. However, a new extreme point is generated because of the overshoot and undershoot phenomena in envelope fitting. Therefore, the decomposition must be performed multiple times. In the second sifting process, the data for processing is h_1 , and the envelope mean is m_{11} . Thus,

$$h_1 - m_{11} = h_{11} \quad (3)$$

The sifting process is repeated k times to obtain

$$h_{1(k-1)} - m_{1k} = h_{1k} \quad (4)$$

Until h_{1k} meets the IMF conditions, the sifting process breaks off. The first IMF is obtained, i.e.,

$$c_1(t) = h_{1k} \quad (5)$$

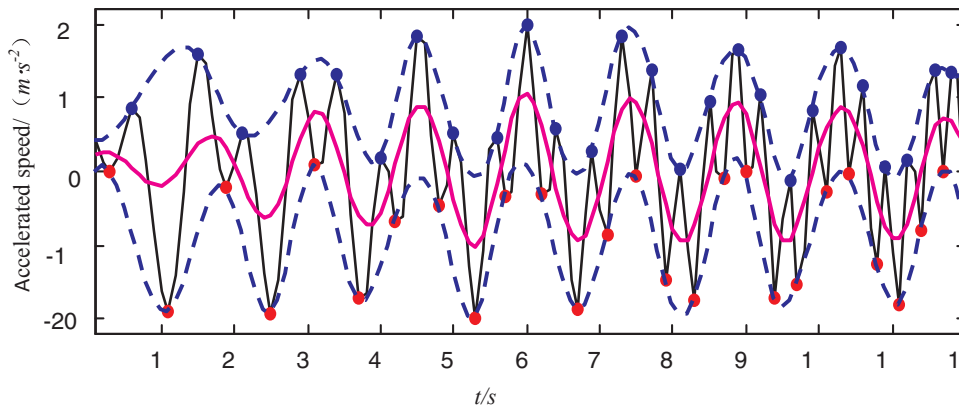


Fig. 2. Acceleration speed response of a mechanical gear vibration test.

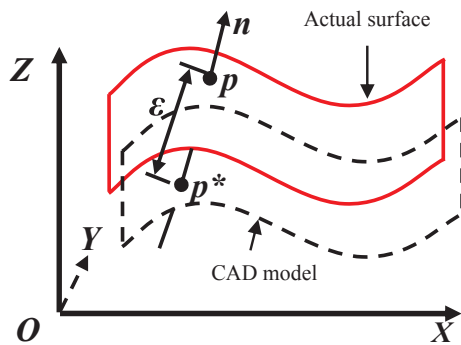


Fig. 3. Surface normal vector direction of the error value.

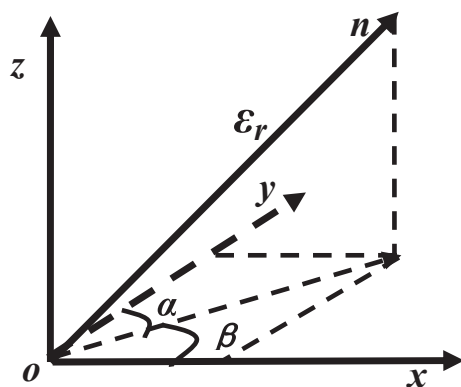


Fig. 4. Compensation component in each axis.

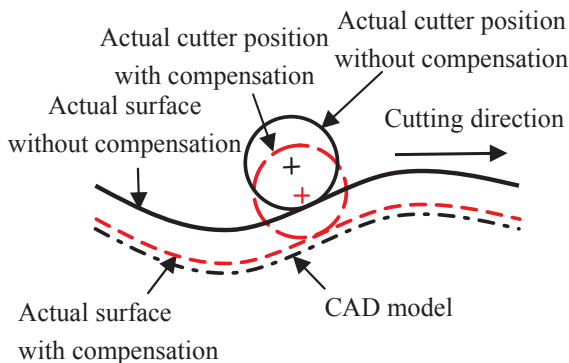


Fig. 5. Comparison of tool path before and after compensation.

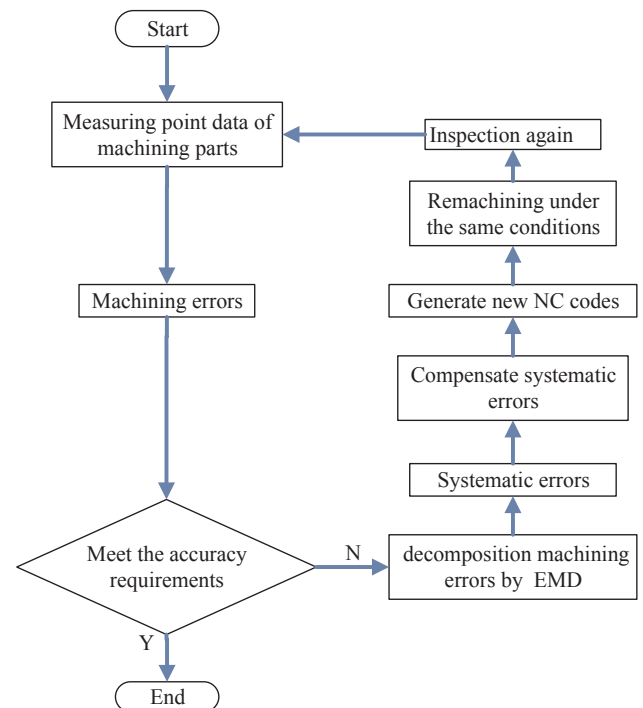


Fig. 6. Flow chart of machining error compensation.

This IMF is the highest frequency in the entire signal data sequence. In the actual decomposition process, the mean m_{1k} of the upper and lower envelopes cannot be zero. A criterion must be determined to halt the sifting process. Thus, Huang et al. proposed the cessation of the sifting criteria as follows:

$$SD = \frac{\sum_0^T |h_{1(k-1)}(t) - h_{1k}(t)|^2}{\sum_0^T |h_{1(k-1)}(t)|^2} \quad (6)$$

When the SD is less than the typical value, the sifting process is stopped. The typical value for SD can be set between 0.2 and 0.3.

(2) Subtracting $c(t)$ from $x(t)$ yields the new data sequence $r(t)$ with the removed high frequency components. Hence,

$$x(t) - c_1(t) = r_1(t) \quad (7)$$

where $r_1(t)$ is treated as the new data $x(t)$, and it is subjected to the same sifting process described above. The IMF $c_2(t), \dots, c_n(t)$ can be obtained during the sifting process until the $r_n(t)$ satisfies the termination condition. By summing up Eqs. (6) and (7), we obtain

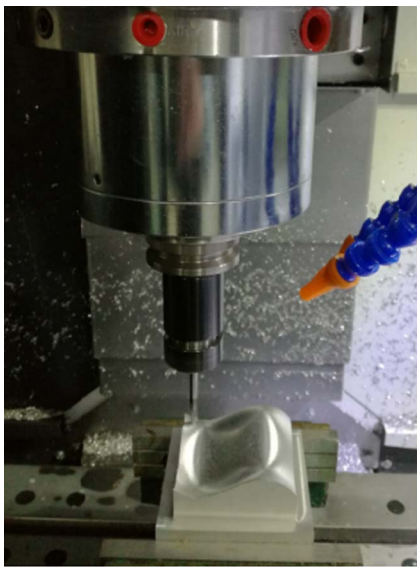
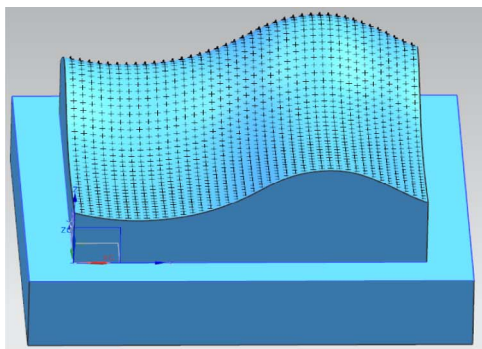


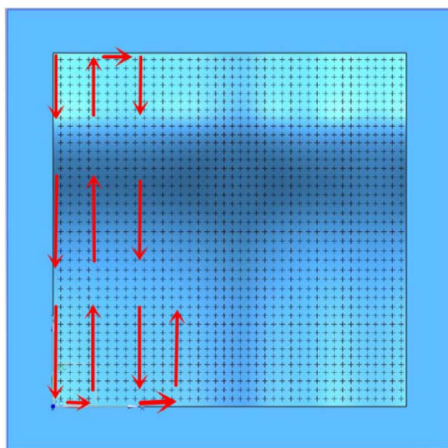
Fig. 7. Machining process of an example surface part.



Fig. 9. Offline inspection of the surface part.



(a) 3-dimensionally distribution of 1600 measured points on the part surface



(b) Measurement path of 1600 measured points on the part surface

Fig. 8. Distribution of the measured points of the surface part.

$$x(t) = \sum_i^n c_i(t) + r_n(t) \tag{8}$$

Thus, the data is decomposed into n intrinsic empirical modes and a residue, which can either be the mean trend or a constant.

The most significant and important information in the original

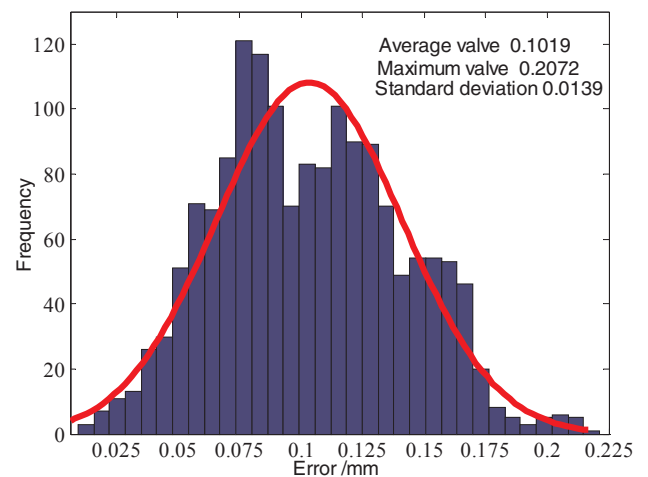


Fig. 10. Histogram of the machining errors of the surface part without compensation.

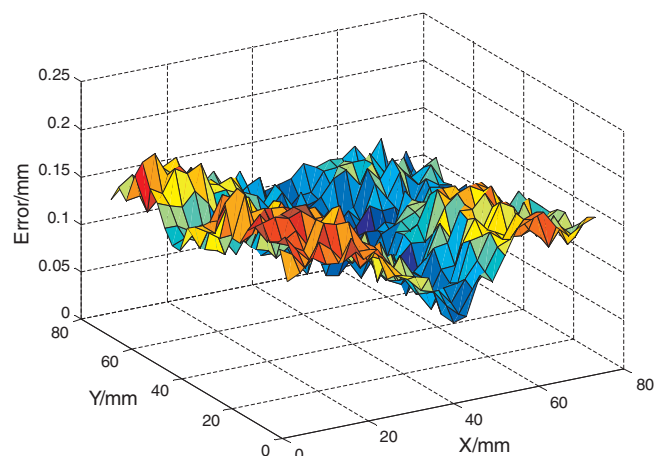


Fig. 11. Distribution of machining errors without compensation.

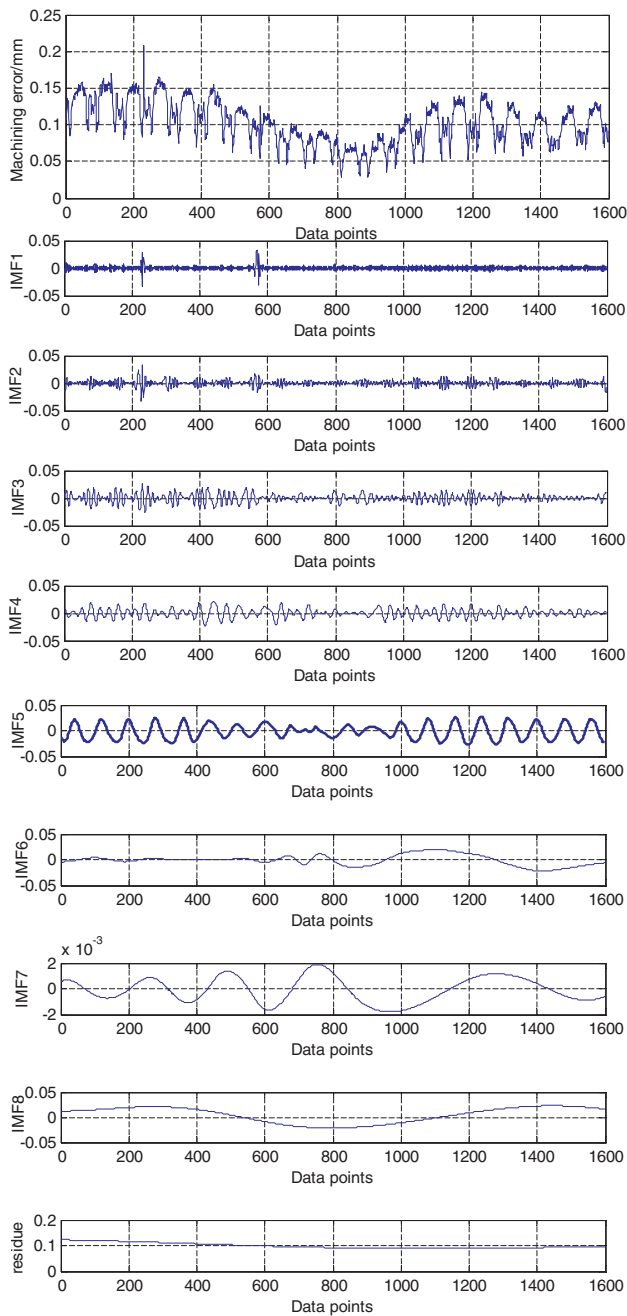


Fig. 12. Results of the machining errors decomposed by EMD.

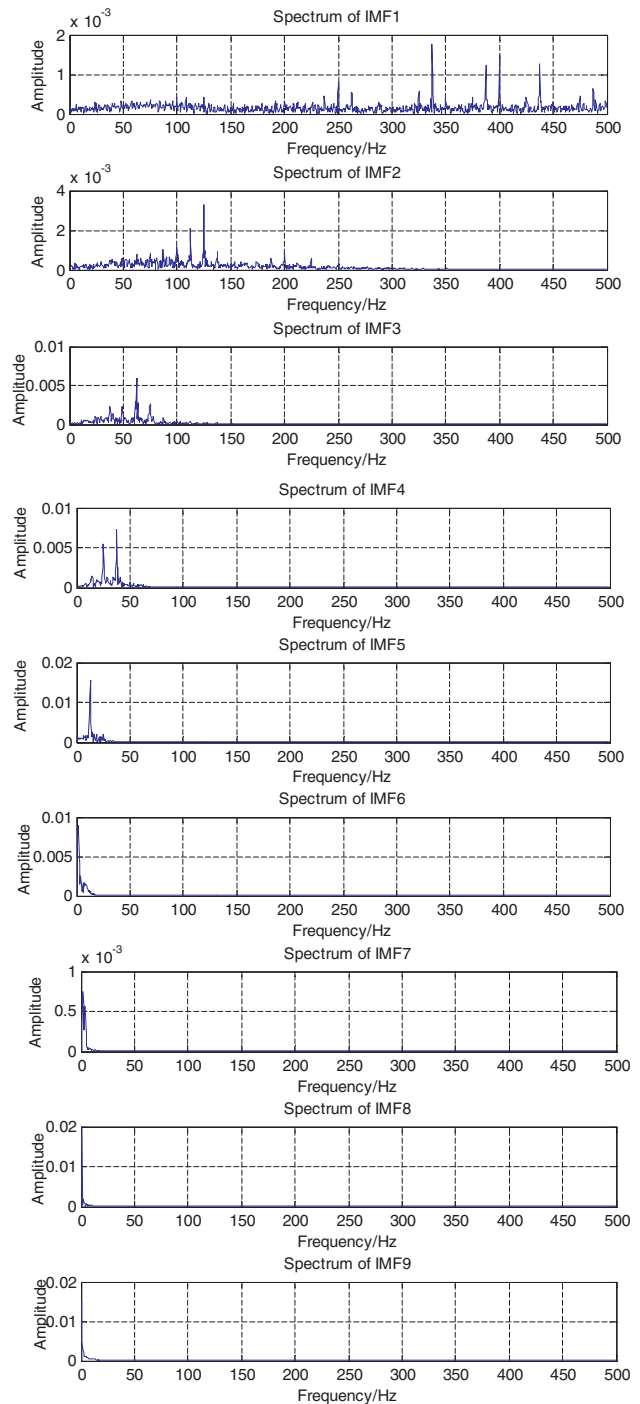


Fig. 13. Spectrum of IMF 1–9.

Table 1
Correlation coefficients of each IMF component.

IMF 1	IMF 2	IMF 3	IMF 4	IMF5	IMF 6	IMF 7	IMF8	IMF9
0.0241	0.0032	0.0829	0.0515	0.0825	0.0959	0.0047	0.1928	0.9178

signal is concentrated in the first few IMF components of EMD decomposition. The trend information in the original signal curve is distributed in the residue [13].

3.2. Systematic error decomposition

Various forms of systematic errors exist, but the changes are regular. Systematic errors can be determined from the IMF components and the residue by analyzing the form of systematic errors. By analyzing various

forms of systematic errors, some systematic error forms must be included in the residue [13,14]. The systematic errors of periodic variation must be determined according to the nature of systematic errors and their deterministic characteristics. At varying frequencies of the IMF components, low-frequency IMF components must be categorized to periodic variation of system errors. However, whether high-frequency IMF components can be categorized to the periodic variation of system errors need to be judged. Autocorrelation and spectral analyses of the IMF component are combined in the current study to extract the cyclical systematic errors. Autocorrelation analysis can be employed to obtain signals in different periods of dependence or similarity [15,16] and to extract the signal cycle. However, when the periodic signal with noise is extracted, the periodic signal must have a high signal-to-noise

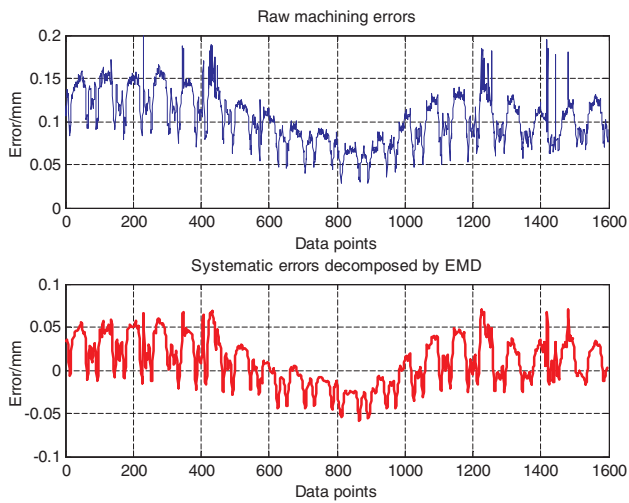


Fig. 14. Comparison of machining and systematic errors.

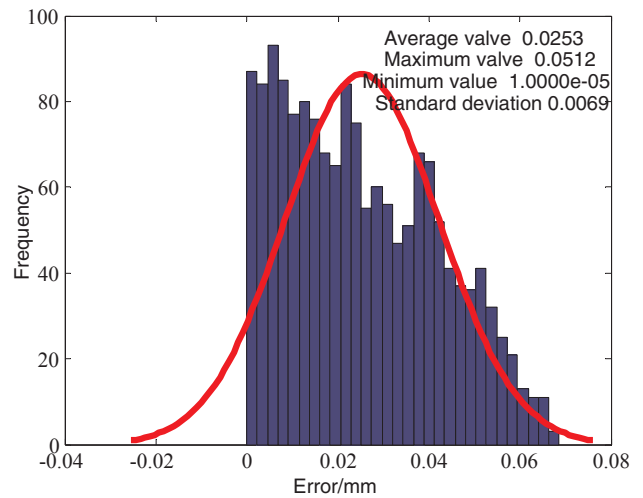


Fig. 16. Histogram of machining errors with EMD compensation.

ratio [17].

The main steps of the correlation coefficient method for the IMF component include determining the correlation coefficient of each IMF component and the original signal. The bigger the correlation coefficient value of IMF component and the original signal is, the bigger the correlation between IMF component and the raw error is, and vice versa. The typical value of the correlation coefficient is 1/10 of the maximum value of the correlation coefficient in the IMF component. If the correlation coefficient is less than the typical value, it is an invalid IMF component. If the correlation coefficient is greater than or equal to the typical value means that the IMF component is effective. However, the correlation coefficient method is less discriminative, and the different effects are not obvious. Thus, the signal near the typical value is easy to miscalculate. In this case, each IMF component is analyzed by spectral analysis to determine whether each IMF component contains periodic systematic errors. Therefore, the decomposition of systematic errors of IMF components is actually the decomposition of small periodic systematic errors. The entire decomposition process includes decomposing the machining errors into several IMF components and into

a residue using EMD. Autocorrelation analysis method is used for each IMF component to determine whether periodic variation systematic errors exist. Finally, spectrum analysis method is used to determine whether each IMF component contains periodic variation systematic errors.

3.3. Decomposition of random errors

The sum of systematic and random errors is the machining errors. In theory, as long as one of the error components is known, the other part of the error component is obtained based on the difference. After separating the systematic error components using the EMD error decomposition method, random errors can be obtained by subtracting systematic errors from machining errors.

4. Compensation of machining errors

The actual positions of the tool center and the relationship between the theoretical positions with the compensation method for the

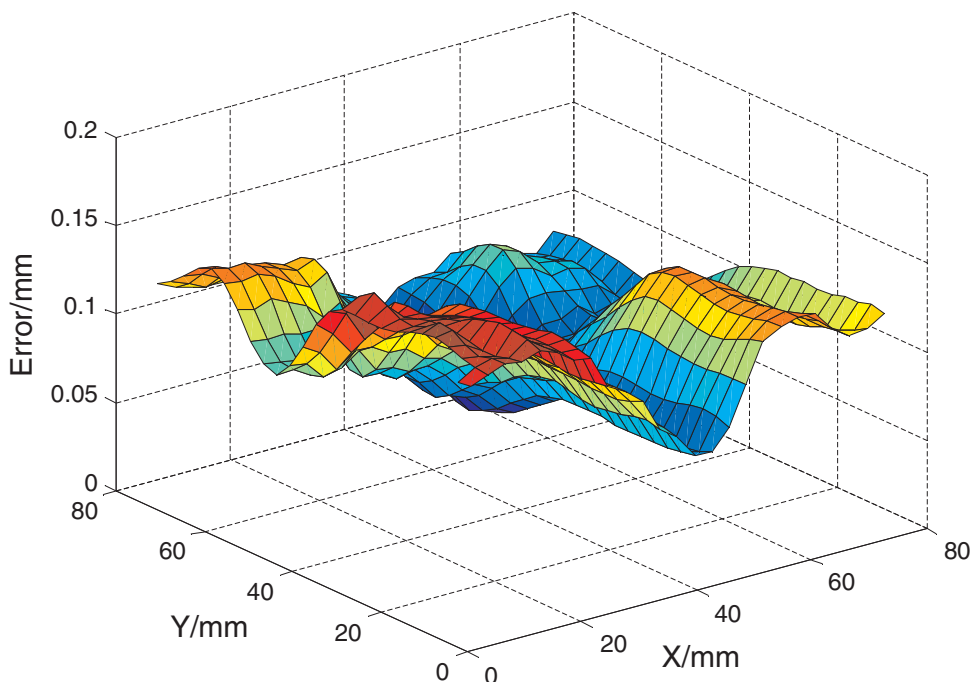


Fig. 15. Distribution of systematic errors decomposed by EMD.

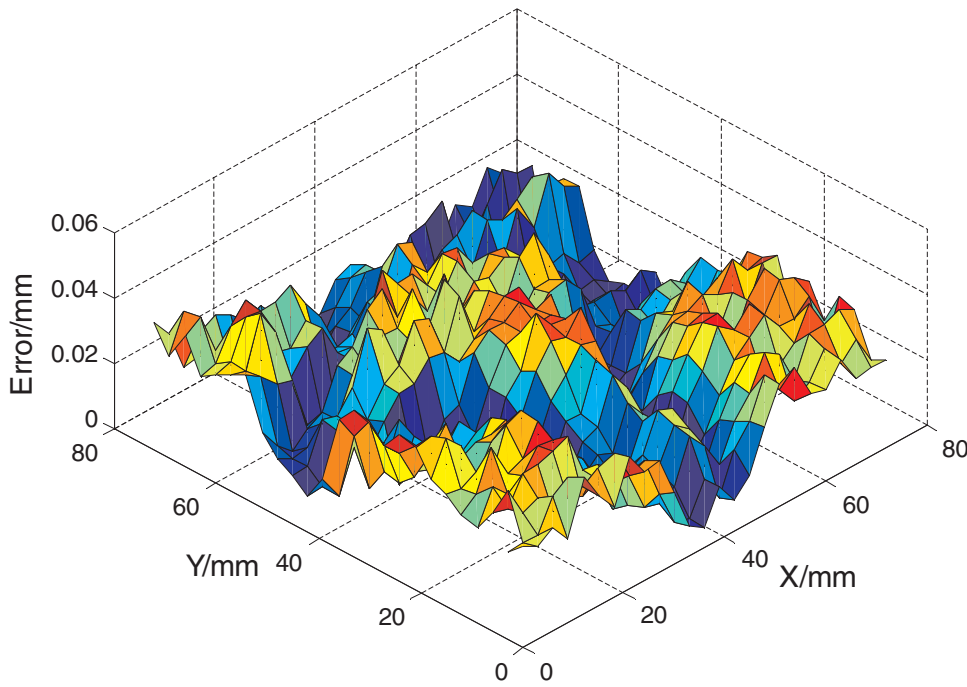


Fig. 17. Distribution of machining errors with EMD compensation.

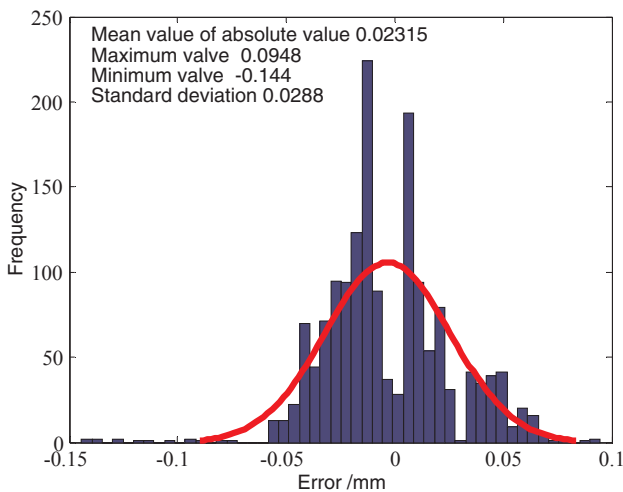


Fig. 18. Histogram of machining errors with origin machining error compensation.

machining errors are determined in the current study. The accuracy of part machining is improved by compensating for the points of a certain quantity. The basic principle of machining compensation technology is offsetting the tool path by a certain distance and processing the part to meet accuracy requirements. The key to machining compensation technology is establishing the relationship between the actual and theoretical positions of the tool center. Surface machining errors are based on the normal vector errors of the actual machining surface shown in Fig. 3. Theoretical point coordinate $p^*(x,y,z)$ is set. The measured point coordinate $p(x',y',z')$ is set. The normal vector of the actual machining surface is $n(u,v,w)$. The distance between the two points is machining error ϵ . The relationship graph corresponding to the amount of compensation in the X, Y, and Z axes is shown in Fig. 4. The amount of compensation ϵ_r in the X, Y, and Z directions is the projection value in the direction normal to the surface along each direction, i.e., $\epsilon_r \cdot u, \epsilon_r \cdot v, \epsilon_r \cdot w$. In this study, the amount of compensation $\epsilon_r \neq \epsilon_x, \epsilon_y$ is the systematic error of the machining error decomposed by EMD. The theoretical position of the tool center is $p^*(x,y,z)$, and the actual machining position of the tool center is $p(x',y',z')$. The relationship

between the two variables is as follows:

$$\begin{cases} x' = x - \epsilon_r \cdot u \\ y' = y - \epsilon_r \cdot v \\ z' = z - \epsilon_r \cdot w \end{cases} \quad (9)$$

When the relationship between the theoretical and actual machining positions and the amount of error compensation is obtained, the data of the inspected points can be compensated. A new theoretical surface is fitted by importing the compensated points to the software UG. The NC code is generated again, and the comparison of the tool path before and after compensation is indicated in Fig. 5. The research program flow of the machining error compensation technology is shown in Fig. 6.

5. Experimental verification

To verify the effectiveness of the compensation method based on EMD in improving the machining accuracy of complex surfaces, a complicated surface part machining experiment was performed. The surface part was inspected offline after the first machining. The inspection accuracy of the offline inspection is high and easy to realize. Thus, the offline inspection scheme was adopted. A coordinate measuring machine (CMM) was used to measure the surface of the machined part. The measurement results were obtained and analyzed. The systematic and random errors among the machining errors were determined through EMD decomposition. Error compensation was used to compensate the systematic errors and to obtain the compensated NC code. According to the NC codes after compensation, the surface part was reprocessed under the same conditions and inspected using the CMM.

The machining device was a three-axis vertical machining center (Fanuc 0i-MD Numerical control system). The part was made of aluminum alloy, and the blank sizes were 100 mm × 100 mm × 60 mm. The NC program for the surface machining was generated by UG.

The finishing cutting conditions were as follows:

- Ball-end cutter diameter: 6 mm;
- Feed rate: 213 mm/min;
- Spindle speed: 3000 r/min;

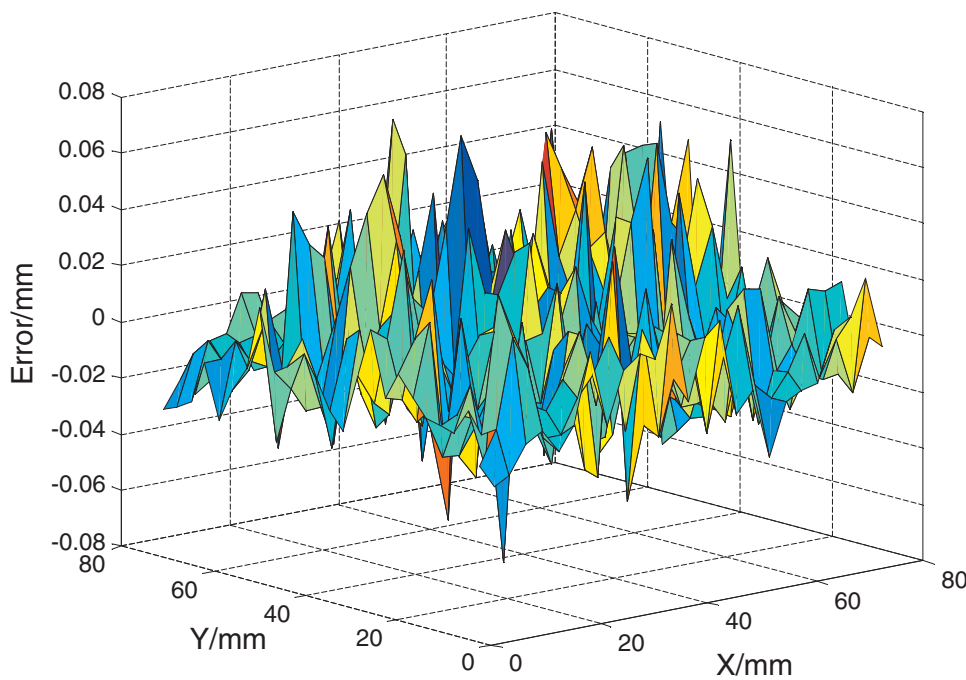


Fig. 19. Distribution of machining errors with origin machining error compensation.

Table 2
The comparison of two methods for machining error compensation/mm.

	EMD compensation	Origin machining error compensation
Average value	0.0253	0.02315
Maximum value	0.0512	0.0948
Minimum value	1.0000e-05	-0.144
Standard deviation	0.0069	0.0288

Tool path: 45-degree line cut method;
Step: residual height mode;
Maximum residual height: 0.003 mm.

The machining process is shown in Fig. 7.

The measurements were carried out on a Hexagon CMM (QUINDOS software, $MPE_E = 0.9 + L/400 \mu\text{m}$), which was equipped with a touch probe with a diameter of 5 mm.

The part was moved to the high-precision measurement table after finishing and then measured by the CMM. The 3-dimensionally distribution of 1600 points on a complex surface is presented in Fig. 8(a). The raw errors distribution of the 1600 measuring points is arranged using the method of head to tail as shown in Fig. 8(b). The measurement process is indicated in Fig. 9. The machining errors of the part surface are obtained based on the measured data. The machining error histogram of the part surface is shown in Fig. 10, and the machining error distribution of the part surface is shown in Fig. 11. Figs. 10 and 11 show that the maximum and average machining errors of the surface are $207.2 \mu\text{m}$ and $101.9 \mu\text{m}$, respectively.

Based on the empirical mode method described in the current study, the machining errors were decomposed in MATLAB as shown in Fig. 12. The machining errors were decomposed into nine IMF components, where IMF 1–8 were the intrinsic mode functions and IMF 9 was the residue, which satisfies the convergence criterion of Formula (6). The correlation coefficients of the IMF 9 components decomposed with the raw machining errors are shown in Table 1. The spectrum of each IMF is indicated in Fig. 13. Table 1 shows that the correlation between the IMF 9 component and the raw machining errors is the largest, and the typical value is 1/10 of the correlation coefficient of IMF 9, i.e., 0.09178. IMF6 and IMF8 contain periodic variation systematic errors; however,

the correlation coefficients of the IMF3, IMF4 and IMF5 components are similar to the typical value. Based on the spectrogram of each IMF component in Fig. 13, the IMF3, IMF4, and IMF5 components contain periodic variation systematic errors. Therefore, according to the content described above, IMF3, IMF4, IMF5, IMF6, IMF8 as well as the residue of IMF components contain systematic errors decomposed by EMD. The comparison between machining and systematic errors and the systematic error distribution are shown in Figs. 14 and 15, respectively

After the machining errors were decomposed into systematic and random errors, the systematic errors were compensated for. Using Formula (9) in MATLAB to modify the theoretical surface of each measurement points, the point cloud was imported into the UG, which regenerated the theoretical surface and CAD model and generated new NC codes. According to the new NC codes, another new work blank was re-machined under the same conditions, and the part surface is inspected again. The machining errors of the processed surface were obtained by analyzing the measured data. The histogram and distribution of the machining errors after compensation are shown in Fig. 16 and Fig. 17, respectively. By comparing Figs. 10 and 16, and Figs. 11 and 17, the average value of machining errors were reduced from $101.9 \mu\text{m}$ to $25.3 \mu\text{m}$, and the maximum error decreased from $207.2 \mu\text{m}$ to $51.2 \mu\text{m}$. Machining accuracy increased by 75.2%. The results indicated that the proposed method can effectively improve machining accuracy.

Actually, the errors after compensation based on systematic errors also include a predominant contribution of the random errors. So the machining errors are not uniformly distributed on the surface. On one hand, the random errors can not be completely decomposed by EMD method. On the other hand, the machining conditions during the compensation process are not just the same as the first machining.

In order to prove that the decomposition process is necessary, a contrast experiment was conducted to compensate the raw machining errors directly under the same machining conditions. The machining error histogram of the part surface is shown in Fig. 18, and the machining error distribution is shown in Fig. 19. Figs. 18 and 19 show that the maximum, minimum, average machining errors of the surface are $71.2 \mu\text{m}$, $-144 \mu\text{m}$ and $23.15 \mu\text{m}$, respectively. And these figures also show that the overcutting occurred result from the undecomposed random errors, which are embraced in compensated errors.

The comparison of two methods for machining error compensation is shown in Table 2. It can be seen that the standard deviation of origin machining error compensation is greater than that of EMD compensation. The random errors have some inevitable effects on error compensation, thus it is necessary to apply the decomposition method to improve part machining accuracy.

6. Conclusions

Machining errors are complex nonlinear and non-stationary signals consisting of systematic and random errors. To improve the machining accuracy of the surface, machining errors were initially decomposed into several IMFs and a residue based on EMD. Systematic errors were detected among the IMF and residue, and they were compensated. Based on the comparison before and after the compensation, the machined surface accuracy after compensation increased by 75.2%. The result verified that EMD and the machining error compensation method significantly improved machining accuracy. The proposed method can be employed without considering complex error sources. The method focuses on the decomposition and compensation of the measurement errors of machining errors, which simplifies the machining error compensation problem.

Acknowledgements

This work was financially supported by the National Nature Science Foundation of China (51565006), the Natural Science Foundation of Guangxi Province (2014GXNSFAA118337), the Science Research Innovation Team Project of Guangxi Provincial Education Department, the Science Research Innovation Team Project of Guangxi University of Science and Technology, and the Guangxi Key Laboratory Director Project (2014JZKG005).

References

[1] E.S. Topal, A cutting force induced error elimination method for turning operations,

- J. Mater. Process. Technol. 170 (1–2) (2005) 192–203.
- [2] Q. Cheng, B. Sun, Z. Liu, et al., Geometric error compensation method based on Floyd algorithm and product of exponential screw theory, Proc. Inst. Mech. Engrs. Part B J. Eng. Manuf. (2016).
- [3] M.W. Cho, G.H. Kim, T.I. Seo, et al., Integrated machining error compensation method using OMM data and modified PNN algorithm, Int. J. Mach. Tools Manuf. 46 (12–13) (2006) 1417–1427.
- [4] M. Poniatowska, Free-form surface machining error compensation applying 3D CAD machining pattern model, Comput. Aided Des. 62 (C) (2015) 227–235.
- [5] Wei Wang, Jian-Guo Yan, Xiao-Dong Yao, et al., Comprehensive modeling and real-time compensation of geometric error and thermal error for CNC machine tools, Chinese J. Mech. Eng. 48 (7) (2012) 165–170 (in Chinese).
- [6] Y. Chen, GAO. On-line inspection and machining error compensation for complex surfaces, J. Mech. Eng. 48(23) (2012) pp. 143–151.
- [7] N.E. Huang, Z. Shen, S.R. Long, et al., The empirical mode decomposition method and the Hilbert spectrum for nonstationary time series analysis, Proc. R. Soc. London 454A (1998) 903–995.
- [8] N.E. Huang, Z. Wu, A review on Hilbert-Huang transform: method and its applications to geophysical studies, Rev. Geophys. 46 (2) (2008).
- [9] O. Niang, A. Thioune, et al., Partial differential equation-based approach for empirical mode decomposition: application on image analysis, IEEE Trans. Image Process. 21 (9) (2012) 3991–4001.
- [10] T.M. Rutkowski, D.P. Mandic, A. Cichocki, A.W. Przybyszewski, EMD approach to multichannel eeg data - the amplitude and phase components clustering analysis, J. Circ. Syst. Comp. 19 (1) (2010) 215–229.
- [11] M.H. Yeh, The complex bidimensional empirical mode decomposition, Signal Processing. 92 (2) (2012) 523–541.
- [12] G. Rilling, P. Flandrin, P. Goncalves, On empirical mode decomposition and its algorithms, in: Proc. IEEE-EURASIP Workshop on Nonlinear Signal and Image Processing NSIP-03. Grado (I)(2003) 3.
- [13] L.I. Shi-Ping, Fu Yu, J. Zhang, Systematic error decomposition method based on EMD, China Measurement & Test, 2011.
- [14] C. Wang, M. Gan, C. Zhu, Non-negative EMD manifold for feature extraction in machinery fault diagnosis, Measurement 70 (2015) 188–202.
- [15] S. Lu, J. Wang, Y. Xue, Study on multi-fractal fault diagnosis based on EMD fusion in hydraulic engineering, Appl. Therm. Eng. 103 (2016) 798–806.
- [16] A.B. Ming, Z.Y. Qin, W. Zhang, et al., Spectrum auto-correlation analysis and its application to fault diagnosis of rolling element bearings, Mech. Syst. Signal Process. 41 (s 1–2) (2013) 141–154.
- [17] C. Guo, Y. Wen, P. Li, et al., Adaptive noise cancellation based on EMD in water-supply pipeline leak inspection, Measurement (2015).